Molecular Crystals and Liquid Crystals

Publication details, including instructions for authors and subscription information:
http://www.tandfonline.com/loi/gmcl20

Compact Lasers Based on HPDLC Gratings

D. E. Lucchetta [a], L. Criante [a], O. Francescangeli [a] & F. Simoni [a]

[a] Dipartimento di Fisica e Ingegneria dei Materiali e del Territorio and Istituto Nazionale per la Fisica della Materia, Università Politecnica delle Marche, Ancona, Italy

Version of record first published: 17 Oct 2011

To cite this article: D. E. Lucchetta, L. Criante, O. Francescangeli & F. Simoni (2005): Compact Lasers Based on HPDLC Gratings, Molecular Crystals and Liquid Crystals, 441:1, 97-109

To link to this article: http://dx.doi.org/10.1080/154214091009581

Mol. Cryst. Liq. Cryst., Vol. 441, pp. 97–109, 2005

ISSN: 1542-1406 print/1563-5287 online
DOI: 10.1080/154214091009581

Taylor & Francis
Taylor & Francis Group

Compact Lasers Based on HPDLC Gratings

D. E. Lucchetta
L. Criante
O. Francescangeli
F. Simoni
Dipartimento di Fisica e Ingegneria dei Materiali e del Territorio and Istituto Nazionale per la Fisica della Materia, Università Politecnica delle Marche, Ancona, Italy

We report the fabrication technique and the main emission properties of two novel all-organic laser devices based on high-resolution reflection gratings written on holographic polymer-dispersed liquid crystal materials by means of conventional holographic techniques. The first type of laser is based upon a distributed Bragg-reflector configuration whereas the second one makes use of a distributed-feedback configuration. Different monomer/liquid-crystal/photoinitiator mixtures are analysed and the main parameters affecting the grating reflectivity and the overall performances of these plastic mirrorless laser device are discussed.

Keywords: distributed Bragg reflectors; distributed feedback; high resolution gratings; organic lasers

1. INTRODUCTION

In recent years, a great interest has grown in the design of compact plastic lasers. Starting from the pioneering works of Kogelnik and Shank [1–2] on distributed feedback (DFB) dye lasers, several different approaches have been used to get laser emission in mirrorless organic devices based on the same operational principles [3–7]. Many of these devices are based on transient gratings, others on permanent high resolution one-dimensional (1D) photonic bandgap (PBG) structures made with a number of different materials. For what concerns the permanent gratings, light amplification phenomena have been

Address correspondence to F. Simoni, Dipartimento di Fisica e Ingegneria dei Materiali e del Territorio and Istituto Nazionale per la Fisica della Materia, Università Politecnica delle Marche, via Brecce Bianche 60131 Ancona (Italy). E-mail: f.simoni@univpm.it

first observed in holographic polymer-dispersed liquid crystals (HPDLC) gratings doped with the coumarine dye [7]. The fabrication techniques and emitting properties have been recently improved leading to the realization of a "one step" DFB organic laser [8]. The possibility of realizing devices based on solid semiconducting conjugated polymers has also been shown in the distributed Bragg reflectors (DBR) geometry [9]. More recently laser emission and electrically controlled wavelength flipping have been demonstrated in photopumped HPDLC plastic lasers based on a DBR configuration [10]. In this work we present a detailed description of the fabrication techniques and a characterization of main emission properties of two organic photopumped light emitting devices based on HPDLC gratings and working in the DBR and DFB geometries.

2. EXPERIMENTAL PART

2.1. Samples

The main part of our two devices is the high resolution reflection grating. It was realized by exposing an isotropic monomer-liquid crystal photo-sensitive mixture for 20 minutes to the interference pattern of two *s*-polarized Ar^{++} ion laser beams. The impinging light intensity was in the range between 40 and 70 mW/cm^2 per beam and the incident angles were selected to obtain a spatial pitch $\Lambda = 0.2\,\mu m$. A small value of the periodicity is an essential requirement to get reflection gratings working in the visible spectral range. The grating wavevector K ($K = 2\pi/\Lambda$) was normal to the glass surfaces. The pre-polymer mixture was a solution of three components, the monomer dipentaerythritol-hydroxy-pentaacrylate (DPHPA), a nematic liquid crystal (NLC) and a solution of the photoinitiator Rose Bengal (RB) and the coinitiator N-phenyglycine (NPG) in the N-vinylpyrrollidone (NVP). Three different mixtures were analyzed: the mixture-A with a ratio between DPHPA:LC:initiator solution of 40:40:20, mixture-B with a ratio of 50:30:20 and mixture-C with a ratio of 50:36:14. The chemical structure of these components was reported elsewhere [11]. Mixture-C was optimized to absorb light in the blue region of the electromagnetic spectrum [18]. To this aim, the amount of NPG was considerably increased (4% in weight of RB and 10% of NPG dissolved in the NVP). Moreover, different LCs (BL001, BL006 and BL038 from Merck) were used to modify the dielectric contrast of the periodic structures. In order to increase the mobility of the reactive groups the sample was heated at a temperature above the glass transition temperature

of the polymer and maintained at that temperature during the entire irradiation process. The optical characterization of the grating was performed by measuring its transmission spectrum. The measurement was carried out by illuminating the grating through an optical fiber with an incoherent tungsten light source emitting in the wavelength range 350–1000 nm, and collecting the transmitted light through an optical fiber connected to a monochromator. In order to get laser emission a frequency-doubled Nd:YAG laser was used as the excitation source (the pump beam). In both configurations the light impinged at 45° to the direction of the grating wave vector, with energy values per pulse in the range between 6.3 μJ and 6.7 mJ ($\tau = 4$ ns, $\lambda =$ 532 nm). The data were then corrected for angle and polarization dependent Fresnel reflection losses. Light emitted from the side of the pump beam in the direction of K was collected and focused by a short-focal length lens into the entrance slit of a spectrometer, displayed, stored and analyzed on a personal computer.

2.2. DBR Configuration

Thee DBR configuration consists of a double layered structure. The first layer is a 1D reflection grating sandwiched between two parallel glasses with a thickness of 23 μm. The second layer contains the photo-active material, i.e., a solution of the Rhodamine 6G in ethanol at concentrations of 10^{-3} or 10^{-4} M sandwiched between two slightly misaligned ITO-coated plane glasses. Using this configuration, the grating can be written and optical characterized before addition of the second layer containing the active material. Samples in the DBR geometry were irradiated at $\lambda_w = 514$ nm and the incident angle was properly selected to obtain reflected wavelengths within the emission spectrum of the rhodamine dye. Gratings written with different wavelengths showed different positions of the reflection maxima as reported in Figure 1. These changes are mainly connected with the corresponding modification of the grating pitch Λ due to the different writing wavelengths [12–13] ($\Lambda = \lambda_W/2 \sin\theta$, with $\lambda_W =$ writing wavelength, and $\theta =$ incident angle). The inset of Figure 1 shows the position of the reflection peaks as a function of the experimentally accessible writing wavelengths. A linear behavior is observed with negligible changes in the position of the peaks, due to the small modifications in the average refractive index of the grating connected to the different absorption of the photoinitiator mixture, at different wavelengths.

The first LC used to write our periodic structures was the BL001 which exhibit an ordinary refractive index of 1.521 and an extraordinary

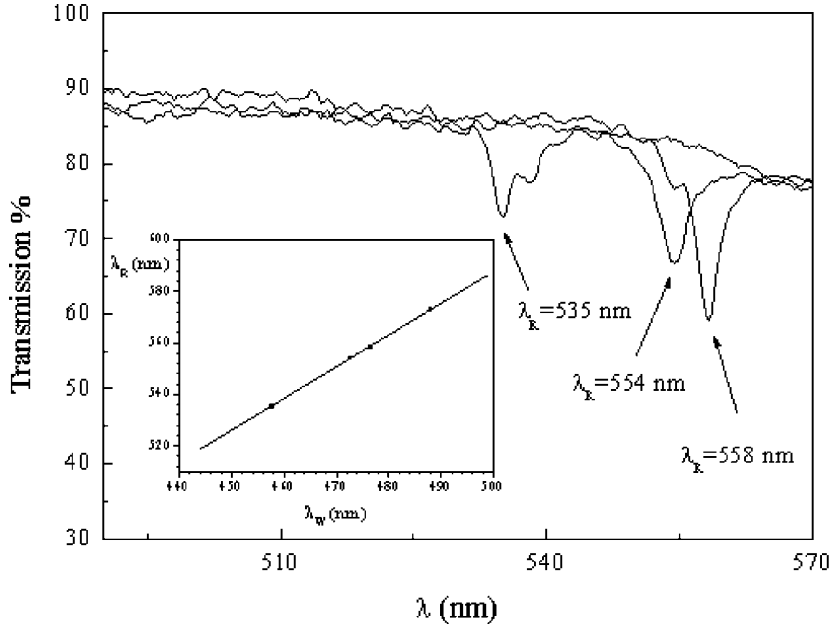

FIGURE 1 Transmission spectra of three reflection gratings written using three different wavelengths ($\lambda_{W1} = 457.8$, $\lambda_{W2} = 472.7$, $\lambda_{W3} = 476.5$). The inset shows the position of the maxima as a function of the used writing wavelengths in a wider wavelength's range.

refractive index of 1.746. Unfortunately, some time the reflectivity of the HPDLC grating was not enough high as expected. According to ref. [14] the reflectivity of a multilayers periodic structure made with two different homogeneous materials increases rapidly with the ratio between their refractive indexes and with the number N of layers.

The last quantity is connected with the grating pitch Λ and as a consequence with the thickness of the periodic structure. To estimate the value of the layer thickness that optimises the reflectivity, we used the results of a theoretical model for propagation of electromagnetic waves in periodic media described in refs. [15,16]. This model can be considered as an extension to the optical wavelengths of the dynamical theory of X-ray diffraction originally developed to describe diffraction effects in perfect crystals. In spite of the relative simplicity, the formalism involved is quite general for periodic homogeneous media. This model shows that a complete coupling between incident and diffracted (reflected in our case) wave settles up over lengths of the periodic

structure corresponding to a few times a characteristic length, called "extinction length." It is defined as:

$$t_{ex} = \frac{\lambda_B \sin\theta_B}{\sqrt{\pi}|\Psi_H|C}$$

where θ_B is the Bragg angle ($\theta_B = \pi/2$ in our case), λ_B is the Bragg wavelength ($\lambda_B = 2n_A \sin\ \theta_B$), C is the polarization factor and Ψ_H is a quantity that measures the strength of the coupling and is defined as

$$\Psi_H = \frac{\Psi_0}{\pi} \quad \text{with } \Psi_0 = \frac{(n_2 - n_1)(n_2 + n_1)}{2n_G}$$

where n_G is the refractive index of the grating, $n_{1/2} = n_G \pm \Delta n/2$ and Δn the grating birefringence. In our case, considering a measured grating birefringence $\Delta n = n_2 - n_1 = 0.004$ [17], a value of the extinction length of about 250 μm can be evaluated. Accordingly, a reflectivity peak close to unity should require an overall thickness of the grating of about 750 μm. This value can be reduced by one order of magnitude by increasing the LC concentration as resulting from the experimental data reported in ref. [18]. However, these calculations must be considered only as a first approximation because the real refractive index profile of the grating is more complicate than the one assumed (i.e., a step profile) and absorption is neglected. According to the above theory, LCs with high optical birefringes and thick samples are required to get a strong reflection peak. Unfortunately, from an experimental point of view it is worth to note than a thick sample (more than 25 μm) tends to absorb more light than a thin one. The first important consequence is that for thick samples, the reflection efficiency of the recorded grating is much lower than expected. In this case the only way we have to increase the reflectivity of the grating is to modify the dielectric contrast between different layers by using new component concentrations (mixture-B and C) and new LCs with higher dielectric anisotropy. In particular in mixture-B we increased the high functional monomer to increase the rate of photopolymerization in order to obtain a well defined periodic structure and in mixture-C the amount of LC was increased to obtain a higher dielectric contrast. In this way the sample thickness can be reduced up to 13 μm without significant changes in the final grating reflectivity and lower voltage values can be applied to the cell if switching is required [19]. Figure 2 reports the typical result for a 50 micron-thick sample made with the mixture-B and LC BL038

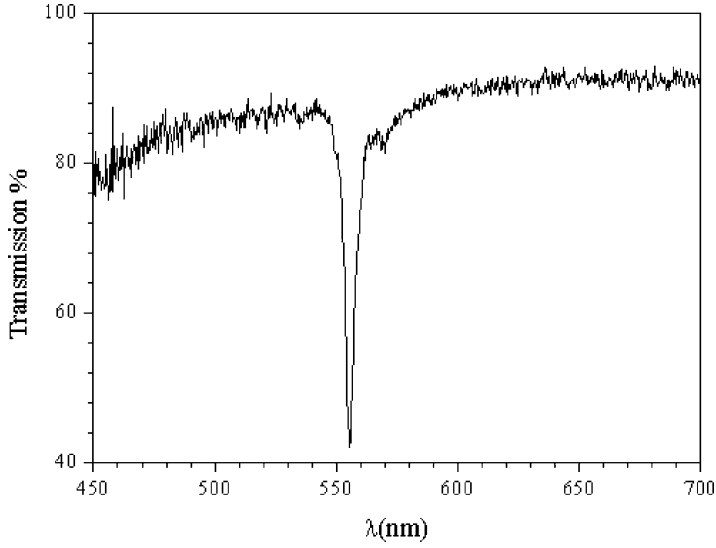

FIGURE 2 Transmission spectra for a 50 micron-thick samples made with the LC BL038 and Mixture-B. Exposure time 15′, light intensity 70 mW/cm^2 per beam, $\lambda_W = 514$ nm.

whose values of the extraordinary refractive indices are $n_e = 1.799$ and $n_o = 1.527$. Similar results deriving from the higher dielectric contrast in the PBG structure were obtained also for the LC BL006 ($n_e = 1.816$ and $n_o = 1.530$). Unfortunately the mixture containing the LC BL006 is unstable becoming practically unusable after few minutes.

In its reflection band the grating works as a distributed Bragg reflector for the laser cavity and the light emitted from the excited dye molecules can be resonantly amplified when the gain condition is fulfilled. When lasing occurs the onset of a narrow peak in the emission spectrum is expected at the correspondent wavelength. Figure 3 shows the emission spectra of the DBR configuration measured when the energy of the pump beam is 1.0 mJ. To make the following discussion clearer, in the same figure it is also shown in dashed line the transmission spectra of the reflection grating used as DBR. The strong narrow peak at 532 nm is the spectral line of the pump source. Laser emission occurs when the pump energy density exceeds the threshold value of 0.4 mJ, as shown by the appearance of a narrow intense peak located approximately at 570 nm, whose linewidth (full width at half maximum, FWHM) is 3 nm. The conversion

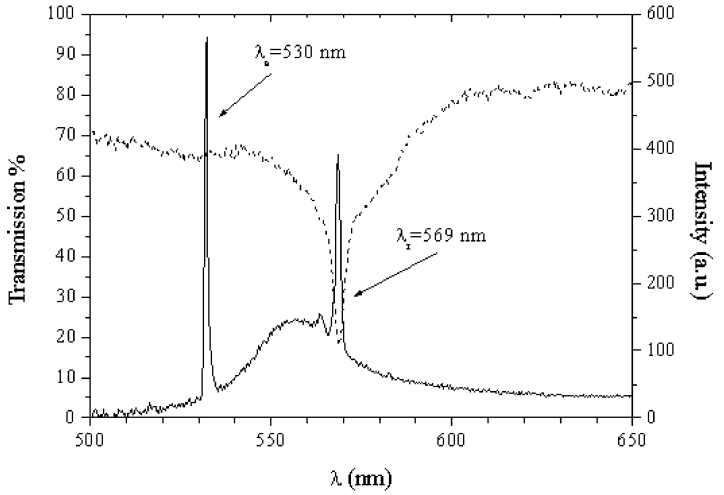

FIGURE 3 Emission spectra of the DBR configuration measured when the energy of the pump beam is equal to 1.0 mJ. In the same figure we have also reported as a dashed line the transmission spectra of the reflection grating used as DBR. The strong narrow peak at 532 nm is the spectral line of the pump source.

efficiency, defined as the ratio of the emitted energy to the impinging one, was measured to be 1% with a pulse length of the laser emission of 4 ns.

This peak occurs at the wavelength where the cavity threshold is minimum according to the usual expression [12]

$$\gamma_{th} = \alpha + \frac{1}{2d}\ln\left(\frac{1}{R_1 R_2}\right)$$

where d is the thickness of the active layer, α a coefficient which represents the volume losses, R_1 and R_2 the reflectivity of the cavity mirrors. If $R_2(\lambda)$ is the grating reflectivity, γ_{th} is minimum in correspondence of the maximum of R_2. This is clearly shown in Figure 3 where the peak of the laser emission corresponds to the grating reflection maximum (i.e., minimum in the transmission spectrum). The emission wavelength of the DBR configuration can be easily tuned in a range of few nanometers by using an external electric field which reorients the LC molecules modifying the average refractive index of the grating structure. Figure 4 shows changes in the transmission spectra of a 23 μm thick reflection grating for different values of the

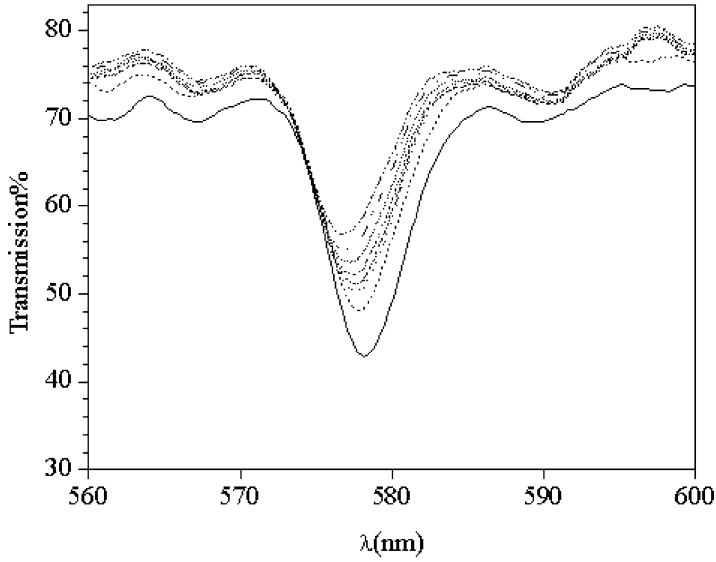

FIGURE 4 Transmission spectra of a HPDLC reflection grating for different values of the applied voltage in the range 0 (lower curve) – 15 (upper curve) V/μm.

applied electric field in the range 0 to 15 V/μm. The electro-optical measurements were carried out by applying for few seconds a sinusoidal electric field with a frequency of 1 KHz to the ITO layers limiting the HPDLC grating. In this particular sample made by mixture-A and LC BL001, when the applied field is zero the grating reflects the wavelength $\lambda_1 = 577$ nm. As expected, with increasing the electric field values up to 10 V/μm a blue-shift of few nanometers of the reflection peak and a simultaneous reduction of the peak amplitude (related to the proximity to the index matching condition) are observed. The emission wavelength follows this behavior until further reductions of the reflectivity of the HPDLC grating bring to a different behavior. In this case the lowest threshold for laser emission does no more occur at the wavelength selected by the HPDLC grating, rather it corresponds to the peak wavelength of the rhodamine emission band ($\lambda_{Rh} = 566$ nm). For this reason switching-off the grating reflectivity by application of a suitable voltage to the HPDLC film allows lasing action at $\lambda_2 = 566$ nm due to the homogeneous character of the emission broadening. In these conditions an interesting effect known as wavelength-flipping (between λ_1 and λ_2) [10] can be observed as reported in Figure 5.

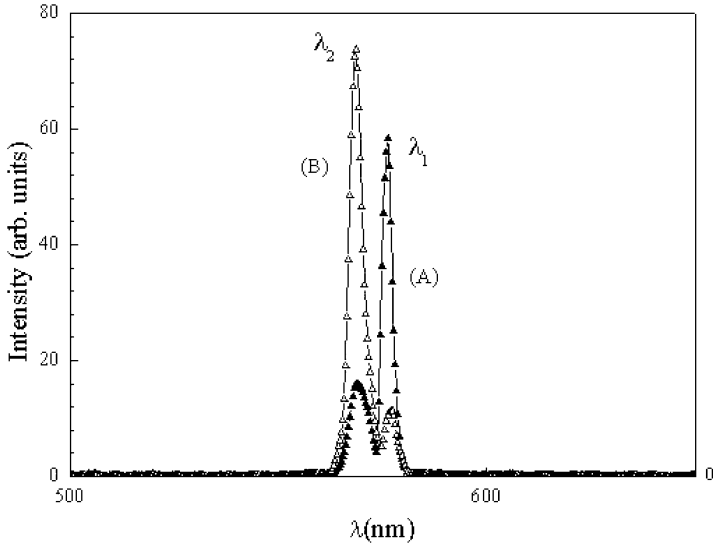

FIGURE 5 Emission spectra of the DBR configuration in the two operational conditions. Curve (a) corresponds to V = 0 Volts ($\lambda_1 = 576\,\text{nm}$), curve (b) corresponds to V = 15 V/μm ($\lambda_2 = 566\,\text{nm}$).

2.3. DFB Configuration

In the DFB arrangement the rhodamine 6G dye is included in the starting mixture at concentrations of 10^{-4} or 10^{-3} M [10] and the gain distributed along the spatial extension of the HPDLC grating after the photopolymerization process. A different writing wavelength $\lambda^* = 476.5\,\text{nm}$ was used to avoid photobleaching of the dye during the sample irradiation. Figure 6 shows the absorption spectra of a 10^{-4} M rhodamine solution (dashed line) and of the mixture of two photoinitiators (continuous line) in the region of interest. In this wavelength range, due to the different absorption properties of these components, a considerable amount of the rhodamine dye remains inside the HPDLC grating after the grating formation allowing gain distribution and amplified spontaneous emission (ASE) when optically pumped. The presence of the rhodamine dye was supported by a spectrometer analysis of Figure 7 in which the transmission spectra of an undoped (empty triangles) and doped (filled triangles) grating are displayed. It is easy to observe a red-shift of the reflection peak when the dye is added to the periodic structure, according to the reflection's law $\lambda_W = 2n_o\Lambda$. The absorption of the rhodamine dye is low but non negligible and the entity of the shift depends on both the initial

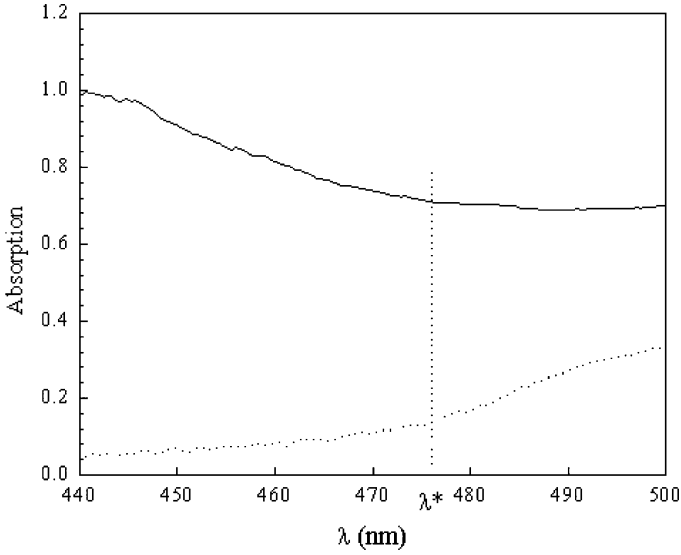

FIGURE 6 Absorption spectra of the rhodamine dye (dashed line) and of the mixture of the photoinitiators RB and NPG (continuous line) dissolved in ethanol. The vertical dashed line indicates the position of the writing wavelength $\lambda^* = 476.5\,\text{nm}$.

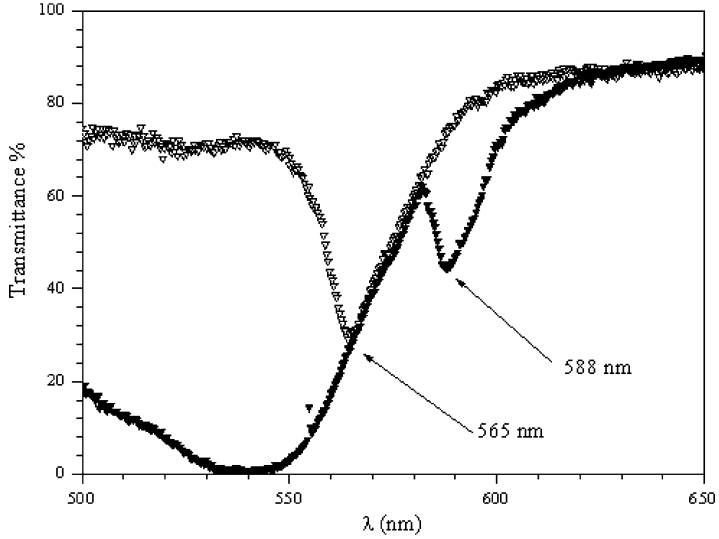

FIGURE 7 Transmission spectra of two 13 μm HPDLC gratings written at $\lambda^* = 476.5\,\text{nm}$ with a light intensity $I = 40\,\text{mW/cm}^2$ x beam. The first grating (empty triangles) doesn't include the rhodamine dye, the second one contains a 10^{-1} M concentration of rhodamine. A red shift of more than 20 nm was observed.

concentration of the dye and exposure time [19]. By using the above described fabrication technique a compact light emitting DFB device can be easily obtained through a simple "one-step" fabrication process as demonstrated in ref [8]. The structure is relatively simple to pump optically and emits a light beam perpendicular to the glass substrates. In its reflection band the grating works as a DFB structure that provides a gain sufficient to observe amplification of the spontaneous emission (ASE) along the optical path. In principle, if the light emitted by the excited dye molecules is resonantly amplified lasing action is possible. When lasing occurs, the onset of a narrow peak in the emission spectrum is expected at a wavelength corresponding to one of the two edges of the PBG [7]. Figure 8 shows one of the emission spectra of a 10 microns DFB device , made with mixture-C, measured when the energy of the pump beam was about 6.7 mJ. The strong narrow peak at 532 nm is the spectral line of the pump source and the peak on the right side of the figure represents the He-Ne laser used to align the cell. In the same figure we have also reported the transmission spectrum of the reflection grating and a magnification (50x) of the emission

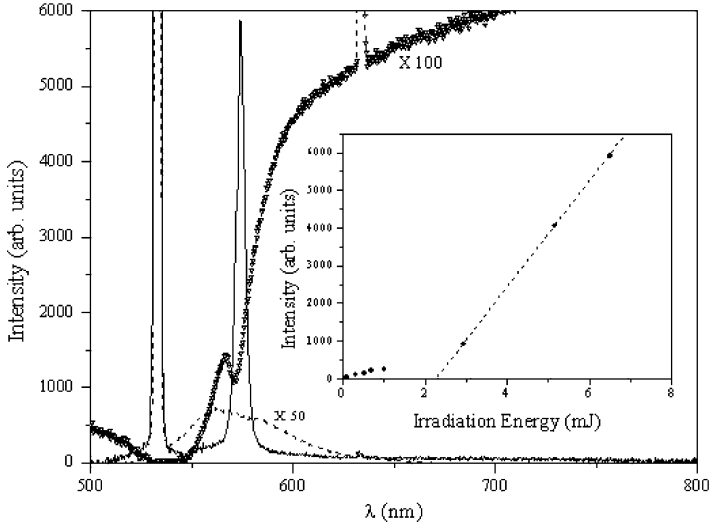

FIGURE 8 Emission spectra of the DFB device for a pump energies 6.7 mJ. The line made of empty triangles corresponds to a 100 x magnification of the transmission spectrum of the HPDLC grating whereas the dashed line on the bottom of the figure represents a 50% magnification of the emission spectrum of the dye mixture for the lowest pumping energy of 6.3 μJ. The peak on the left side represents the excitation wavelength at 532 nm. The inset shows the ASE peak intensity as a function of the irradiation energy.

spectrum of the device when the pump energy is low (6.3 μJ). It is worth noting that the emission band corresponding to the current concentration of the rhodamine dye has a maximum at about 563 nm when pumped with a Nd:YAG laser whereas light amplification is centered around 573 nm. It means that the presence of the high resolution grating selects the wavelength and drives the light emission if the reflection peak falls inside the emission band of the rhodamine dye.

In a more general situation, above a threshold value when the gain condition for laser emission is fulfilled, the light emitted from the excited dye molecules can be resonantly amplified and laser emission occurs. In this situation, the main peak of the structure becomes narrow and intense. In our device, narrowing of the ASE approaching laser emission can be easily observed monitoring the behavior of the main peak as a function of the pump energy [20]. The results are reported in the inset of Figure 9. Analysis of this figure shows that the ASE peak intensity increases nonlinearly with increasing irradiation energy as reported in reference [8]. According to the experimental observations reported in several works [21,22] and to the evidence of a similar behavior observed in comparable systems [8], the narrow (FWHM of 4 nm) peak and the abrupt change observed around 2.0 mJ could reasonably associated with a low Q laser emission with a measured conversion efficiency of about 5%. Photo damage of the dye can affect the performance of the laser devices. In particular the lifetime of the DFB laser strongly depends on the pump energy. In our case the pump energy is relatively low due to the low value of the laser threshold. With such pump energy levels we did not observe significant dye degradation effects. Instead we observed photo degradation when using repeated pulses with an energy density two orders of magnitude higher than that used in the actual experiments.

3. CONCLUSIONS

We have reported the methods to use high-resolution reflection gratings based on HPDLCs to build up compact novel DBR and DFB lasers. The realization of a double-layered DBR structure represented the first step towards realization of a one-step compact DFB laser in which the active media is fully integrated in the periodic structure. The fabrication of a DFB photonic device able to select and amplify the spontaneous emission of the rhodamine 6G has been shown. Different mixtures have been used and the main parameters affecting the grating reflectivity have been discussed. The improvements in the grating fabrication techniques allowed a reduction of the lasing threshold values and strongly increased the lifetime of the DFB

device. We believe that by improving the design of the lasing structures new photonic devices could be fabricated in different geometries leading to new optical devices.

REFERENCES

[1] Kogelnik, H. & Shank, C. V. (1971). *Appl. Phys. Lett*., *18*(4), 152.
[2] Shank, C. V., Bjorkholm, J. E., & Kogelnik, H. (1971). *Appl. Phys. Lett*., *18*(9), 395.
[3] Meier, M., Mekis, A., Dodabalapur, A., Timko, A., Slusher, R. E., Joannopoulos, J. D., & Nalamasu, O. (1999). *Appl. Phys. Lett*., *74*(1), 7–9.
[4] Maillou, T., Le Moigne, J., Geffroy, B., Lorin, A., Rosilio, A., Dumarcher, V., Rocha, L., Denis, C., Fiorini, C., & Nunzi, J.-M. (2001). *Syntetic Metals*, *124*, 87–89.
[5] Rocha, L., Dumarcher, V., Denis, C., Raimond, P., Fiorini, C., & Nunzi, J.-M. (2001). *J. Appl. Phys*., *28*(5), 3067–3069.
[6] McGehee, M. D., Díaz-García, M. A., Hide, F., Gupta, R., Miller, E. K., Moses, D., & Heeger, A. J. (1998). *Appl. Phys. Lett*., *72*(13), 1536–1538.
[7] Jakubiak, R., Bunning, T. J., Vaia, R. A., Natarajan, L. V., & Tondiglia, V. P. (2003). *Adv. Mat*., *15*, 241–244.
[8] Lucchetta, D. E., Criante, L., Francescangeli, O., & Simoni, F. (2004). *Appl. Phys. Lett*., *84*(24), 4893–4895.
[9] Tessler, N., Denton, G. J., & Fried, R. H. (1996). *Nature*, *382*, 695–697.
[10] Lucchetta, D. E., Criante, L., Francescangeli, O., & Simoni, F. (2004). *Appl. Phys. Lett*., *84*(6), 837–839.
[11] Sutherland, R. L., Natarajan, L. V., Tondiglia, V. P., & Bunning, T. J. (1993). *Chem. Mater*., *5*, 1533.
[12] Yariv, A. (1991). "*Optical Electronics*," 4e International edition, Saunders College Publishing.
[13] Eichler, H. J., Günter, P., & Pohl, D. W. (1985). "*Laser-Induced Dynamic Gratings*," Springer-Verlag.
[14] Born, M. & Wolf, E. (1980). "*Electromagnetic Theory of Propagation Interference and Diffraction of Light*," Pergamon Press.
[15] Francescangeli, O., Melone, S., & De Leo, R. (1989). *Phys. Rev. A*, *40*(9), 4988–4996.
[16] Francescangeli, O., Melone, S., & De Leo, R. (1991). *Phys. Rev. A*, *43*(12), 6975–6989.
[17] Lucchetta, D. E., Criante, L., & Simoni, F. (2003). *Opt. Lett*., *28*(9), 725–727.
[18] Lucchetta, D. E., Criante, L., & Simoni, F. (2003). *J. of Appl. Phys*., *93*(12), 9669–9674.
[19] Lucchetta, D. E. et al. *Unpublished results*
[20] Tsutsumi, N., Kawahira, T., & Sakai, W. (2003). *Appl. Phys. Lett*., *83*(13), 2533–2535.
[21] Anni, M. & Pisignano, D. (2003). *Synthetic Metals*, *137*, 1057–1058.
[22] Zavelani-Rossi, M. et al. (2003). *Synthetic Metals*, *139*, 901–903.